Targeted and random mutagenesis of cassava brown streak disease susceptibility factors reveal molecular determinants of disease severity

ZJ Daniel Lin[1,3], Myia K. Stanton[1], Gabriela L. Hernandez[1], Elizabeth J. De Meyer[1], Zachary von Behren[1], Katherine Benza[1,2], Helene Tiley[1], Anna Meirink[1], Emerald Hood[1], Greg Jensen[1], Kerrigan B. Gilbert[1], James C. Carrington[1], Rebecca S. Bart[1]

1. Donald Danforth Plant Science Center, Saint Louis, MO 63132, USA
2. Washington University, Saint Louis, MO 63130, USA
3. corresponding author: ZDL: dlin@danforthcenter.org

Abstract

Cassava brown streak disease (CBSD) is caused by cassava brown streak viruses (CBSVs) from the family *Potyviridae*. Potyvirid viral genome-linked protein (VPg) recruitment of host eukaryotic translation initiation factor 4E (eIF4E) proteins is a critical step in the viral life cycle. CBSV VPg interacts with all five cassava eIF4E-family members. Simultaneously knocking out *eIF4E*-family genes *nCBP-1* and *nCBP-2*, in cultivar 60444, strongly reduces CBSD root symptoms and viral titer but does not result in complete resistance, likely due to gene family redundancy. To test for redundancy, we generated single and double mutants for each clade of the *eIF4E* gene family in farmer preferred cultivar TME419. Double mutants for the *eIF(iso)4E* and *nCBP* clades both exhibited reduced symptom severity, with *ncbp-1 ncbp-2* having the strongest phenotype. A yeast two-hybrid screen for nCBP-2 mutants that lose VPg affinity identified fifty-one mutants, including an L51F mutant. This finding is consistent with one of the recovered cassava mutants that had a 6 amino acid deletion, including L51, in nCBP-2 and showed a reduction in symptoms relative to wild type. The data presented here suggest that generating mutations corresponding to L51F of nCBP-2 in multiple or all five cassava eIF4E proteins may lead to stronger resistance to CBSD while avoiding pleiotropic effects.

Keywords

Cassava brown streak disease, *Potyviridae*, eIF4E, viral genome-linked protein (VPg), gene editing, yeast two-hybrid

Introduction: 717
Results: 1,845
Discussion: 1,519
Materials & Methods: 1,263

Introduction

Cassava is one of the most important starch crops grown in the world (*Agricultural production statistics 2000–2022*, 2023). In sub-Saharan Africa, cassava is particularly important for food security, but its production is threatened by viral diseases (Rey & Vanderschuren, 2017). In particular, cassava brown streak virus (CBSV) and Ugandan cassava brown streak virus (UCBSV), closely related ipomoviruses belonging to the family *Potyviridae*, are of major concern (Tomlinson *et al.*, 2018; Robson *et al.*, 2023). Independent or simultaneous infection by these viruses cause cassava brown streak disease (CBSD). Symptoms of CBSD include feathery chlorosis of leaves, brown streaking of stems, and necrosis of storage roots. Cassava varieties with varying levels of resistance have been identified and are being deployed, but none of the varieties currently available to farmers are fully immune (Sheat & Winter, 2023; Robson *et al.*, 2023). A highly effective RNAi-based transgenic approach has been developed but faces regulatory hurdles in many target countries (Odipio *et al.*, 2014; Beyene *et al.*, 2016; Wagaba *et al.*, 2016; Tomlinson *et al.*, 2018).

Viruses of *Potyviridae* are positive sense, single stranded RNA viruses (Valli *et al.*, 2015). Many of these viruses have been studied extensively as a large number are agronomically important pests (Revers & García, 2015; Yang *et al.*, 2021). In many potyvirus-plant pathosystems, members of the host *eIF4E* gene family function as susceptibility factors and are necessary for completion of the viral life cycle (Robaglia & Caranta, 2006; Naderpour *et al.*, 2010; Hart & Griffiths, 2013; Bastet *et al.*, 2017; Gomez *et al.*, 2019; Gao *et al.*, 2020). This gene family encodes mRNA cap-binding proteins that facilitate recruitment of translation machinery to transcripts (Browning & Bailey-Serres, 2015). The plant *eIF4E*-family can be broken into three clades: *eIF4E*, *eIF(iso)4E*, and *nCBP* (Gomez *et al.*, 2019). Previous work in *Arabidopsis* demonstrated that turnip mosaic virus (TuMV) requires a functional copy of *eIF(iso)4E* for disease (Duprat *et al.*, 2002). Since then, potyvirus resistance loci in many crops have been mapped to *eIF4E*-family genes and alleles conferring potyvirus resistance often harbor missense mutations (Bastet *et al.*, 2017). Additional studies have demonstrated that potyvirid viral protein genome-linked (VPg) interacts with eIF4E-family proteins (Wittmann *et al.*, 1997; Schaad *et al.*, 2000) confirming that the interacting *eIF4E*-family member functions as a susceptibility factor (Yeam *et al.*, 2007; Charron *et al.*, 2008). Conversely, viral isolates that break *eIF4E*-family based resistance have been found to have accumulated compensating mutations in their VPg (Charron *et al.*, 2008; Gallois *et al.*, 2010; Li *et al.*, 2016; Lebaron *et al.*, 2016; Takakura *et al.*, 2018). VPg is covalently linked to the 5' end of the viral genome. It has been hypothesized that VPg interacts with eIF4E-family proteins to recruit translational machinery to synthesize the viral polypeptide (Sanfaçon, 2015) and complete the viral life cycle. Solving the structure of VPg-susceptibility factor protein complex could facilitate

76 engineering of susceptibility factor alleles that cannot be co-opted by the pathogen. However,
77 co-crystal structures have yet to be produced and the VPg protein complex with eIF4E-family
78 *S* factors falls below the current minimum size limit required for cryogenic electron microscopy.
79 To date, engineering synthetic *eIF4E* resistance alleles has involved transferring resistance-
80 conferring mutations from one pathosystem to another with some degree of success (Kim *et*
81 *al.*, 2014; Bastet *et al.*, 2018, 2019; Zafirov *et al.*, 2021).
82 We previously found that simultaneous mutations in two cassava eIF4E-family
83 members, *nCBP-1* and *nCBP-2,* strongly attenuated CBSD storage root necrosis and
84 accumulation of CBSV in storage roots of cultivar 60444 (Gomez *et al.*, 2019). Knocking out
85 *nCBP-2* alone resulted in an intermediate phenotype, while the *ncbp-1* single mutant exhibited
86 no differences from wild type. Aerial symptoms persisted in the *ncbp-1 ncbp-2* double mutant,
87 although with less severe stem brown streaking. This incomplete resistance suggests that VPg
88 may interact broadly with the remaining cassava eIF4E-family proteins. Indeed, CBSV VPg
89 could associate with all five cassava eIF4E-family proteins by coimmunoprecipitation (Gomez
90 *et al.*, 2019). As full CBSD resistance may require engineering all cassava *eIF4E*-family
91 alleles to evade CBSV VPg, we employed targeted and random mutagenesis of nCBP-2 to
92 identify structural determinants of VPg interaction. Furthermore, to better understand the
93 degree of functional redundancy exhibited by cassava eIF4E-family proteins in CBSD, we here
94 expand our CRISPR/Cas enabled genetic approach to characterize the roles of cassava eIF4E
95 and eIF(iso)4E clades in CBSD.
96
97 **Results**
98 **Generation of cassava *eIF4E*-family mutants**
99 We previously reported that a cassava *ncbp-1 ncbp-2* double mutant in the 60444
100 background displayed increased, but incomplete, resistance to CBSV challenge (Taylor *et al.*,
101 2012; Gomez *et al.*, 2019). While VPg interacted most strongly with nCBP-1 and nCBP-2 in
102 yeast two-hybrid assays, all five eIF4E-family proteins interacted with VPg in co-
103 immunoprecipitation assays. These results suggest that there is likely functional redundancy
104 among this family of proteins. To test this idea, we used CRISPR/Cas9-mediated genome
105 editing to generate new cassava *eIF4E*-family mutants in TME419, a farmer preferred cassava
106 cultivar. gRNAs were designed to target the first exon of each target gene and cassava
107 transformations were performed as previously described (Fig. S2) (Taylor *et al.*, 2012; Gomez
108 *et al.*, 2019). A total of 156 recovered lines from 21 transformations were characterized for
109 possible mutations at the target site(s) using amplicon sequencing. These efforts yielded
110 independent single mutant lines for all members of the cassava *eIF4E* gene family, along with
111 *eif(iso)4e-1 eif(iso)4e-2* and *ncbp-1 ncbp-2* double mutants (Table 1, S3). All but one mutant
112 line used in this study are predicted to have frameshifting mutations that result in loss of protein

113 function. The lone exception is one of the *ncbp-1 ncbp-2* double mutants where both *nCBP-1*
114 alleles and one allele of *nCBP-2* have frameshifting mutations and the remaining *nCBP-2*
115 allele has a deletion that results in loss of amino acids 45 through 51. This allele is designated
116 *nCBP-2*^{K45_L51del} and the mutant line is designated *ncbp-1 nCBP-2*^{K45_L51del} (Table 1, S3). No
117 differences in growth and development were observed between any of the mutant lines and
118 wild type (Fig. S3-4).
119
120 **CBSD phenotypes of TME419 *eIF4E*-family mutants**
121 To determine the contribution of cassava *eIF4E* family genes to development of CBSD,
122 mutant and wild type TME419 were challenged with CBSV isolate Naliendele in greenhouse
123 trials where stem brown streaking and leaf feathery chlorosis were tracked for approximately
124 three months. The specific CBSV isolate was chosen as it produces strong aerial symptoms
125 quickly after inoculation and reliably results in strong storage root necrosis (Wagaba *et al.*,
126 2013). At the end of the viral challenges, storage roots were excavated from soil, sectioned,
127 and scored for severity of necrosis as a measure of spread along storage root length and
128 diameter (Gomez *et al.*, 2019). These same root samples were used to measure viral titer by
129 quantitative real-time PCR (qRT-PCR). For aboveground symptoms, *eif4e*, *eif(iso)4e-1,*
130 *eif(iso)4e-2,* and *ncbp-1* single mutants had no reduction in disease severity relative to wild
131 type, while *ncbp*-2 and both *eif(iso)4e* and *ncbp* double mutants exhibited small but significant
132 reductions (Figure 1a). For storage root necrosis symptoms in the single mutants, the *ncbp-1*
133 and *ncbp-2* mutants displayed a decrease in symptoms compared to wild type with the latter
134 showing the strongest phenotype (Figure 1b). Each of the double mutants showed a decrease
135 in symptom with the *ncbp-1 ncbp-2* mutant, where all *nCBP* alleles have frameshifting
136 mutations, having the greatest reduction in necrosis; virtually no necrosis was observed
137 (Figure 1b, d, S5_). We further measured viral accumulation in storage roots of wild type,
138 *ncbp-1*, *ncbp-2*, *ncbp-1 ncbp-2*, and *ncbp-1 nCBP-2*^{K45_L51del} lines using qPCR analysis and
139 observed that lines with frameshifting mutations in *ncbp-2* had significantly lower virus titer
140 (Figure 1c). Taken together, these data suggest that while nCBP-2 is the primary contributor
141 to root disease severity, other eIF4E-family members may also contribute throughout the plant.
142
143 **Purified CBSV VPg and cassava eIF4E-family proteins interact *in vitro***
144 To further explore functional redundancy within the eIF4E-family with respect to CBSD
145 and, specifically, interaction with VPg, we used a biochemical approach. Using co-
146 immunoprecipitation, we previously demonstrated that CBSV VPg and cassava eIF4E-family
147 proteins form complexes in whole cell lysates using co-immunoprecipitation (Gomez *et al.*,
148 2019). However, these experiments did not address whether the proteins are directly
149 interacting or if another complex member is present and facilitating the protein-protein

150 association. Thus, we tested if VPg directly associates with eIF4E-family proteins in the
151 absence of additional factors using a GST pull-down experiment. GST-tagged cassava eIF4E-
152 family proteins and VPg, tagged with both 6xHis and 3xFLAG, were expressed in and purified
153 from *E. coli* (Figure S6). We found that CBSV VPg was pulled down by GST-tagged eIF4E,
154 nCBP-1, and nCBP-2 in comparison to GST alone (Figure 2a, b). Pulldown of VPg by GST-
155 tagged eIF(iso)4E-1 and eIF(iso)4E-2 was also tested but we observed inconsistent
156 enrichment of VPg by GST-eIF(iso)4E-1 & -2, relative to GST alone, across experimental
157 replicates.
158
159 **Targeted nCBP-2 mutations fail to disrupt interaction with VPg**
160 If CBSV VPg can coopt all cassava eIF4E-family proteins for completing the viral
161 lifecycle, engineering cassava to be resistant to CBSV may require identifying alleles of *eIF4E*-
162 family genes encoding mutations that disrupt VPg binding but still allow for translation-initiation
163 activity. In other plant-potyvirid pathosystems, specific mutations within eIF4E-family members
164 have proved sufficient to block interaction with VPg while maintaining normal protein function
165 (Figure 2c) (Ashby *et al.*, 2011; Kim *et al.*, 2014). One well studied example is TuMV VPg and
166 *Arabidopsis* eIF(iso)4E. In this system, mutation of a highly conserved tryptophan (W92L) and
167 semi-conserved lysine (K149E) in *Arabidopsis* eIF(iso)4E disrupts binding of TuMV VPg in
168 pull-down and co-immunoprecipitation experiments. Overexpression of this mutant *eIF(iso)4E*
169 allele in Chinese cabbage confers resistance to TuMV (Miyoshi *et al.*, 2006; Kim *et al.*, 2014).
170 To test the hypothesis that specific *eIF4E* gene family alleles might avoid VPg binding, we
171 took a yeast two-hybrid approach using different alleles of *nCBP-2*. We recapitulated the
172 W92L/K149E mutations from Arabidopsis eIF(iso)4E in cassava nCBP-2, resulting in nCBP-
173 $2^{W118L/N170E}$ (Figure 2d). Whereas the eIF(iso)$4E^{W92L/K149E}$ no longer associated with TuMV VPg
174 in a co-immunoprecipitation experiment (Figure 2e), we observed that CBSV VPg was
175 similarly present in both wild type nCBP-2 and nCBP-$2^{W118L/N170E}$ pull downs (Figure 2f). VPg
176 - nCBP-$2^{W118L/N170E}$ interaction was also observed through yeast two-hybrid assay (Figure 2g,
177 h).
178 TuMV and CBSV belong to two different genera of *Potyviridae*, *Potyvirus* and
179 *Ipomovirus*. It is possible that viruses from these distinct genera have evolved mechanistic
180 differences in how their VPg proteins interact with host eIF4E-family *S* factors. To determine
181 VPg protein conservation between potyviruses and ipomoviruses, VPg sequences from five
182 major potyvirus clades were aligned with VPg sequences from seven of the eight known
183 ipomovirus species (TomMMoV, SPMMV, SqVYV, CocMoV, CVYV, UCBSV, CBSV) (Figure
184 S7). Across all VPg sequences analyzed, several highly conserved residues are observed, as
185 are striking genus-specific differences; four stretches of amino acids are present only in one
186 genus or the other (pink boxes). One of these stretches coincides with an α-α loop in PVY VPg

187 thought to directly interact with the ventral side of eIF4E (Coutinho de Oliveira *et al.*, 2019); in
188 ipomoviruses this region is eight amino acids shorter. Additionally, a highly conserved
189 aspartate residue (D77) necessary for TuMV VPg interaction with *Arabidopsis* eIF(iso)4E
190 (Léonard *et al.*, 2000), is not present in ipomoviruses, indicating this residue may have a less
191 conserved role in interactions between ipomovirus VPgs and eIF4E-family proteins.
192
193 **A yeast two-hybrid screen identifies nCBP-2 mutants that lose VPg affinity**
194 Since mutations from the known Arabidopsis resistance allele did not block nCBP-2 –
195 VPg interaction, we performed a yeast two-hybrid screen for nCBP-2 mutants that lose affinity
196 for VPg (Figure 3a). Mutant *nCBP-2* amplicons were generated by error-prone PCR and
197 cloned into the bait vector by *in vivo* recombination in EGY48 yeast already containing both
198 *lacZ* reporter and VPg prey vectors (Figure 3a). From roughly 1000 yeast transformants, 51
199 *nCBP-2* mutants were isolated that lost interaction with VPg (Table 2, Table S4). Forty-eight
200 unique amino acid substitutions were observed across forty-six unique nCBP-2 mutants. Of
201 the unique mutants, 27 had mutations affecting a single residue or the introduction of a
202 frameshifting deletion while 19 contained two or three mutated residues. Nine residues were
203 isolated more than once, with up to three unique amino acid substitutions identified. Mutants
204 were then filtered to identify residues with varying degrees of conservation (Figure S8) across
205 cassava eIF4E-family proteins resulting in 15 being re-cloned and validated for loss of VPg
206 interaction in yeast using a quantitative β-galactosidase activity assay. All but two mutants,
207 nCBP-2^{L147H} and nCBP-2^{R196S}, were confirmed to confer total loss of β-galactosidase activity
208 in yeast and suggest commensurate loss of VPg affinity (Figure 3b, 5b, S9). The R196S
209 mutant yeast did not have any reduction of β-galactosidase activity relative to yeast expressing
210 wild-type nCBP-2, while L147H mutant yeast exhibited an intermediate reduction in β-
211 galactosidase activity. We further validated by western blot analysis that the yeast used for
212 two-hybrid experiments expressed nCBP-2 variants and CBSV VPg (Figure S9).
213
214 **Translation initiation activity of isolated nCBP-2 mutants**
215 Previous work with *Arabidopsis eif4e* or *eif(iso)4e* mutants suggested that both genes
216 were functionally redundant for translation initiation. However, *eif4e* mutants exhibit subtle
217 reductions in fertility and biomass in addition to delayed flowering time (Bastet *et al.*, 2017,
218 2018). Similarly, simultaneous knockout of tomato *eIF4E1* and *eIF4E2* incurs a growth penalty
219 (Gauffier *et al.*, 2016). T93C is a yeast *eif4e* mutant with chromosomal *eIF4E* replaced with
220 *LEU2* (Altmann *et al.*, 1989). This yeast strain can survive on galactose media due to a
221 plasmid-based *eIF4E* gene that is galactose inducible but is repressed in the presence of
222 glucose (Figure 4a). Coding sequences of nCBP-2 mutants confirmed to lose affinity for CBSV
223 VPg by quantitative yeast two-hybrid were cloned into pG1.1 under control of the constitutive

224 yeast GPD promoter and transformed into T93C. Transfer of these T93C transformants from
225 galactose- to glucose-containing media revealed that only three nCBP-2 mutants rescue loss
226 of *eif4e*: nCBP-2$^{A20T/H94Q/L200P}$, nCBP-2^{L51F}, and nCBP-2^{S138P} (Figure 4bc, 5cd).
227
228 **Mutating the conserved HPL motif of nCBP-2 can affect VPg binding and disease**
229 Among the three nCBP-2 mutants that retained translation initiation activity, nCBP-
230 2^{L51F} stood out as having a mutation in the highly conserved HPL motif. In yeast, this motif
231 participates in docking with eIF4G (Grüner *et al.*, 2016, 2018). In addition, this amino acid is
232 deleted in the nCBP-2^{K45_L51del} cassava mutant line that displayed increased resistance to
233 CBSD (Figure 5a). The HPL motif is found in many plant eIF4E-family proteins and as such,
234 a mutation of the leucine may be suitable for engineering resistance to other potyvirids. We
235 tested the nCBP-2^{K45_L51del} mutant for interaction with VPg by quantitative yeast two-hybrid.
236 Yeast expressing this mutant exhibited no β-galactosidase activity, like yeast expressing
237 nCBP-2^{L51F} (Figure 5b, S10). We confirmed this implied loss of VPg interaction by observing
238 strongly reduced VPg binding in GST pulldowns with both mutant proteins (Figure 6).
239 However, comparing wild-type nCBP-2, nCBP-2^{L51F} and nCBP-2^{K45_L51del} for translation
240 initiation activity in T93C yeast (Δ*eif4e*) showed that while nCBP-2^{L51F} was able to rescue loss
241 of *eIF4E* in T93C it was to a lesser degree than wild type nCBP-2, and nCBP-2^{K45_L51del} was
242 not able to complement T93C (Figure 5c, d).
243 **Mutating the HPL motif of other eIF4E-family proteins also disrupts VPg interaction**
244 We also tested the effects of mutating the HPL motif on VPg interaction for the
245 remaining cassava eIF4E-family proteins. Previously, we observed by yeast two-hybrid that
246 CBSV VPg interaction with eIF(iso)4E-1 and eIF(iso)4E-2 is weak when compared to
247 interaction with nCBPs (Gomez *et al.*, 2019). Detecting these weak interactions requires
248 incubating yeast for at least two days on solid growth media, in contrast to five hours of
249 incubation in liquid media to detect interaction between nCBP-2 and VPg. All cassava eIF4E-
250 family proteins and their HPL to HPF mutants were co-expressed in yeast on solid media for
251 two days and then analyzed by quantitative β-galactosidase activity assay. nCBP-1^{L46F},
252 eIF(iso)4E-1^{L27F}, and eIF(iso)4E-2^{L27F} all exhibited reduced interaction with CBSV VPg
253 compared to their wild type counterparts (Figure 7a, b). However, nCBP-1^{L46F} was found to
254 not be expressed, while eIF(iso)4E-1^{L27F} consistently accumulated to lower levels relative to
255 eIF(iso)4E-1 across experiments (Figure S11). eIF(iso)4E-2^{L27F} accumulated to similar levels
256 relative to wild type protein. nCBP-1^{L46F} and eIF(iso)4E-2^{L27F} were then tested for their ability
257 to rescue T93C *eif4e* yeast. eIF(iso)4E-2^{L27F} was able to rescue T93C, while nCBP-1^{L46F} could
258 not, consistent with lack of nCBP-1^{L46F} accumulation in yeast two-hybrid experiments (Figure
259 7c).

260 Leucine 51 of nCBP-2 corresponds to leucine 28 within *Arabidopsis* eIF(iso)4E. We
261 hypothesized that recapitulating the L51F substitution in *Arabidopsis* eIF(iso)4E could have
262 similar effects on TuMV VPg binding. When we tested this through quantitative yeast two-
263 hybrid assays we observed that the L28F mutation strongly disrupted eIF(iso)4E interaction
264 with TuMV VPg (Figure S12a). However, *Arabidopsis* eIF(iso)4E^{L28F} was not able to rescue
265 T93C *eif4e* mutant yeast (Figure S12b, c).
266
267 **Discussion**
268 *Potyviridae* is the largest plant-infecting family of RNA viruses comprised of 249
269 viruses across 12 genera (Walker *et al.*, 2022). The genus *Potyvirus* is perhaps the best
270 studied as it contains 206 of the 249 known viruses belonging to the family *Potyviridae*. In
271 comparison, only eight species of viruses belonging to the genus *Ipomovirus* have been
272 identified and much less is known about molecular ipomovirus-host interactions (Dombrovsky
273 *et al.*, 2014). While the genome structure and genes encoded by potyviruses and ipomoviruses
274 are similar, and thus it is reasonable to expect a degree of conservation in virulence strategies,
275 it is also likely that differences have arisen given the evolutionary divergence of the two
276 genera. For CBSV in particular, we note that while eIF4E-family proteins are clear
277 susceptibility factors, the breadth of family members that contribute to disease appears
278 broader than typically found for potyviruses (Bastet *et al.*, 2017). Furthermore, while
279 resistance-conferring amino acid substitutions in eIF4E-family proteins have been effectively
280 transferred between potyvirus-pathosystems, we find in this study that *Arabidopsis* eIF(iso)4E
281 mutations that break TuMV VPg interaction fail to do so for the cassava nCBP-2 interaction
282 with CBSV VPg. These observations highlight the need for further characterization of
283 ipomovirus-host molecular interactions.
284 Structure-function analysis of VPg interaction with eIF4E-family susceptibility factors
285 would strongly benefit from crystal or cryo-EM structures of the complex; these have yet to be
286 successfully generated (Coutinho de Oliveira *et al.*, 2019). Most recently, an NMR approach
287 solved the structure of PVY VPg (Coutinho de Oliveira *et al.*, 2019). The PVY VPg and human
288 eIF4E interaction interface was also mapped through monitoring chemical shift perturbations
289 of either protein during NMR spectroscopy. It is unclear how well these findings will translate
290 to diverse potyvirid VPg interactions with cognate plant eIF4E-family proteins, especially for
291 the plant specific eIF(iso)4E clade and considering significant divergence of ipomovirus VPg
292 sequences from those of potyviruses. Thus far, attempts to design *eIF4E*-family resistance
293 alleles have relied on inference-based approaches (German-Retana *et al.*, 2008; Ashby *et al.*,
294 2011; Kim *et al.*, 2014; Bastet *et al.*, 2018, 2019; Zafirov *et al.*, 2021). In contrast, here we
295 utilize a loss-of-affinity screen of randomly mutagenized nCBP-2 variants to identify key
296 residues necessary for interaction with CBSV VPg. Only three nCBP-2 amino acid residues

297 that we found to be necessary for interaction with VPg had previously been described in
298 potyvirus-plant pathosystems. These amino acid residues, D106, V164, and R168 in nCBP-2,
299 are highly conserved across eIF4E-family proteins. In pepper, the *pvr1*^{2} allele of *eIF4E* is
300 responsible for resistance to isolates of PVY and TEV, and the amino acid corresponding to
301 nCBP-2 D106 is one of three causal amino acid substitutions (Kang *et al.*, 2005). That
302 aspartate in pvr1^{2} is substituted with asparagine (D to N). For cassava nCBP-2, two separate
303 D106 substitutions were observed; D106V and D106H, the latter of which co-occurred with an
304 A41T substitution. Only the nCBP-2^{D106V} mutant was tested for translation initiation activity and
305 was found deficient in rescuing T93C *eif4e* yeast. It is unclear if a D106N mutation in nCBP-
306 2, as found in pvr1^{2}, would similarly break VPg interaction while preserving its translation
307 initiation activity. nCBP-2 V164, where mutation to leucine disrupts CBSV VPg interaction,
308 corresponds to V167 in eIF4E of pea. The pea eIF4E^{V167A} variant confers resistance to PSbMV
309 and can rescue *eif4e* yeast. In contrast, cassava nCBP-2^{V164L} does not rescue T93C *eif4e*
310 yeast. Whether the V164A mutation in nCBP-2 would have the same effects as in pea eIF4E
311 is an open question. Lastly, for nCBP-2 R168, the previously described NMR structural study
312 demonstrated that corresponding residues in human eIF4E and wheat eIF(iso)4E are involved
313 in the interaction with *Potato virus Y* VPg (Coutinho de Oliveira *et al.*, 2019). Like nCBP-2^{D016V}
314 and nCBP-2^{V164L}, nCBP-2^{R168C} also failed to rescue T93C.
315 Of the fourteen nCBP-2 loss-of-VPg-interaction mutants that we tested for translation
316 initiation activity, eleven were nonfunctional. The three nCBP-2 variants that retained function
317 were nCBP-2$^{A20T/H94Q/A148V}$, nCBP-2^{L51F}, and nCBP-2^{S138P}. For nCBP-2 $^{A20T/H94Q/A148V}$, A20
318 resides outside of the conserved core of eIF4E family proteins while H94 and A148 are present
319 in alpha helices found on the dorsal side of nCBP-2; further work is required to identify which
320 individual or combination of these amino acids are required for CBSV VPg interaction. S138
321 is similarly located in a dorsal alpha helix while L51 is closer to the dorsal side and located N-
322 terminal of a beta strand. Evidence from a study on PVY VPg interaction with human eIF4E
323 indicates that VPg interfaces with the ventral side of eIF4E (Coutinho de Oliveira *et al.*, 2019).
324 If this also applies to CBSV VPg interaction with nCBP-2, the four aforementioned amino acid
325 residues likely affect VPg binding in an indirect manner. Of particular importance for this study,
326 the L51F substitution impacts the HPL motif, which was also affected in our cassava *ncbp-1*
327 *nCBP-2*^{K45_L51del} line. This led us to test the importance of that motif for CBSD symptom
328 severity. Unlike nCBP-2^{L51F}, nCBP-2^{K45_L51del} did not rescue T93C *eif4e* deficient yeast.
329 Surprisingly, despite the inability to strongly interact with VPg and complement *eif4e* activity,
330 the *ncbp-1 nCBP-2*^{K45_L51del} root disease phenotype was intermediate to wild type and *ncbp-1*
331 *ncbp-2*, indicating that this mutant version of *nCBP-2* is sufficient for the development of some
332 disease symptoms. A similar result has also been observed in pea *eIF4E* mutants where of
333 eight mutants unable to rescue *eif4e* mutant yeast, two were still able to confer susceptibility

334 to PsbMV (Ashby *et al.*, 2011). In such mutants, it may be that low levels of residual translation
335 initiation activity are sufficient for completion of the viral life cycle. Lastly, we note that in a
336 more sensitive yeast two-hybrid assay, while VPg interaction with nCBP-2^{L51F} resulted in eight-
337 fold less reporter activity than with nCBP-2, the strength of this interaction appeared similar to
338 that with eIF(iso)4E-1. This suggests that mutating additional nCBP-2 residues may be
339 necessary for total elimination of VPg binding and for optimal resistance *in planta*.
340 In cassava, the eIF4E-family has five members, and we previously demonstrated that
341 all five proteins interact with CBSV VPg by co-immunoprecipitation (Gomez *et al.*, 2019). We
342 now find, through pulldown experiments with purified proteins, that nCBP-1, nCBP-2, and
343 eIF4E can directly interact with CBSV VPg. This validates our approach for identifying nCBP-
344 2 residues crucial for VPg interaction. In contrast, our pulldown experiments with VPg and
345 eIF(iso)4E-1 and -2 yielded inconsistent results across experimental replicates. This is difficult
346 to interpret, though it is possible that levels of recombinant protein activity vary between
347 purified batches. Further optimization of purification conditions for cassava eIF(iso)4E-1 and -
348 2 may resolve this issue. Regardless, our *in vitro* data lay the groundwork for a more granular
349 investigation of differences in cassava eIF4E-family protein affinity for CBSV VPg; this may be
350 achieved using techniques like surface plasmon resonance or isothermal titration calorimetry
351 (Upadhyay et al., 2024).
352 To determine the contribution of each *eIF4E*-family gene to CBSV symptoms, and
353 therefore the biological relevance of interaction with VPg, we have used CRISPR/Cas9 to
354 generate single mutants of all five genes, as well as some double mutants, in cassava variety
355 TME419. Notably, the *ncbp* double mutant has near total reduction of storage root necrosis,
356 commensurate with strong reductions in viral titer. Of the two *nCBP* genes, *nCBP-2* appears
357 to be the main driver for the improved disease response as evidenced by the results of the
358 single *nCBP* mutants, and that *nCBP-2* is more highly expressed than *nCBP-1* (Gomez *et al.*,
359 2019). As noted in our previous work, the expression difference between *nCBP-2* and *nCBP-*
360 *1* is even more pronounced in storage roots and may be the reason for differential disease
361 response in roots and aerial tissues of *ncbp-2* and *ncbp-1 ncbp-2* mutants (Gomez *et al.*,
362 2019). The disease data are consistent between mutants in both 60444 (Gomez *et al.*, 2019)
363 and TME419. Beyond the *nCBP* clade, the *eIF(iso)4E* clade appears to have a small
364 contribution to disease as aerial symptom severity and storage root necrosis is slightly reduced
365 when both *eIF(iso)4E-1* and *eIF(iso)4E-2* are simultaneously knocked out. This finding also
366 argues against the *ncbp-1 ncbp-2* root disease phenotype being simply due to additively
367 knocking out family members. It remains to be seen if higher order mutant combinations would
368 have an even greater effect on reducing CBSD disease severity. It will also be important to
369 test the utility of *ncbp-1 ncbp-2* mediated resistance against the natural diversity of cassava
370 brown streak viruses in field trials.

371 A key consideration going forward is that any benefits conferred by mutations in eIF4E-
372 family proteins with respect to viral resistance may also be accompanied by growth and
373 developmental penalties (Gauffier *et al.*, 2016, Bastet *et al.*, 2017). Of the four residues
374 identified in *nCBP-2* mutants that may avoid this penalty, three (L51, H94, and A148) are
375 conserved within all cassava eIF4E-family proteins, and the fourth (S138) is conserved within
376 three members. Targeted base editing of some or all of these residues across the entire eIF4E-
377 family may allow for improved CBSV response while maintaining essential protein translation
378 functions. Indeed, we demonstrate here that transferring the L51F mutation from *nCBP-2* into
379 cassava and *Arabidopsis* eIF(iso)4E proteins results in loss of affinity for corresponding VPgs.
380 As base editing approaches mature alongside improvements with gene targeting, combining
381 these approaches with loss-of-VPg interaction screens may facilitate isolation and
382 implementation of novel *eIF4E*-family resistance alleles.
383
384 **Materials and Methods**
385 **Plasmid vector construction**
386 gRNAs for CRISPR/Cas9-based mutagenesis of cassava *eIF4E*-family genes were
387 selected using the CRISPOR webtool (Concordet & Haeussler, 2018). Cas-OFFinder was
388 then used to screen gRNAs for off-target activity against a TME419 reference based genome
389 assembly produced using data (SRX1393295) from Bredeson et al. and the AM560-2 v6.0
390 reference genome (Table S1) (Bae *et al.*, 2014; Bredeson *et al.*, 2016). gRNAs with off-targets
391 containing less than 2-mismatches were excluded from consideration. Finally, gRNAs were
392 cloned into the pDIRECT 21C CRISPR binary vector as previously described by (Čermák *et*
393 *al.*, 2017).
394
395 **Plant transformation, genotyping, and growth parameters**
396 Cassava cultivar TME419 was transformed as previously described (Veley *et al.*,
397 2023). DNA was extracted from recovered transformants using the CTAB procedure. PCR
398 was then used to amplify 240 to 428 bp regions encompassing the gRNA binding sites. Purified
399 amplicons were sent to GENEWIZ for amplicon sequencing. Amplicon sequencing data was
400 analyzed using the CRIS.py python program (Connelly & Pruett-Miller, 2019). Plantlets of
401 transgenic lines were then maintained in tissue culture (Taylor *et al.*, 2012).
402
403 **Viral challenge and disease phenotyping**
404 Cassava disease challenges with CBSV isolate Naliendele, including inoculation,
405 aerial and below ground disease severity assessments, and qPCR-based quantification of
406 storage root viral titer, were carried out as described previously (Gomez *et al.*, 2019). For data
407 analysis, wild type disease severity was compared across all challenges and no significant

408 differences were found (Figure S1). Data for all challenges were then aggregated to increase
409 sample sizes for statistical analysis.
410
411 **Co-immunoprecipitation and GST-pulldown experiments**
412 Co-immunoprecipitation was performed as described previously (Gomez *et al.*, 2019).
413 For GST-pulldown experiments, cassava *eIF4E*-family genes in pENTR/D-TOPO, from
414 Gomez et al., were cloned into pDEST15 (Invitrogen) by Gateway recombination (Invitrogen).
415 pDEST15 encoding cassava *eIF4E*-family genes and pGEX-4T-1 (encoding unfused GST,
416 Cytiva) were transformed into BL21-AI E. coli (Invitrogen) and transformants were used to
417 start overnight seed cultures. Seed cultures were then used to inoculate 250 mL of LB broth.
418 Once inoculated cultures were grown to an OD600 of 0.4, IPTG (pGEX-4T-1) or arabinose
419 (pDEST15) were added to final concentrations of 0.5 mM or 0.2%, respectively, to induce
420 recombinant protein production. Induced cells were incubated for four hours at 28°C. Cells
421 were then pelleted and resuspended in 4 mL of lysis buffer (125 mM Tris, 150 mM NaCl, 1
422 mM DTT, 5 mM $MgCl_2$, 10 mM $CaCl_2$, pH 7.4) supplemented with 1X cOmplete protease
423 inhibitor (EDTA-free, Roche). Lysozyme (GoldBio) was added to a concentration of 1 mg/mL
424 and the mixture was allowed to incubate at room temperature for 15 minutes. 50 uL DNAse I
425 (Thermo) was then added to the mixture, followed by sonication on ice to ensure complete
426 lysis and elimination of DNA induced viscosity. The resulting cell lysate was centrifuged at
427 4°C, maximum speed, for 20 minutes. 3.5 mL of clarified lysate was transferred to a new tube
428 and EDTA was added to a final concentration of 1 mM. GST and GST-eIF4E proteins were
429 then purified from clarified lysate using glutathione magnetic agarose beads (Pierce)
430 according to manufacturer's protocol. Glutathione was removed from GST and GST-fusion
431 protein eluates by buffer exchange with Amicon Ultra centrifugal filters (Millipore). CBSV
432 6xHis-VPg-3xFLAG-6xHIS was produced and purified for pulldown experiments as described
433 in (Gomez *et al.*, 2019). GST pulldown was performed by mixing 3 ug of GST or GST-eIF4E
434 proteins with 3 ug of VPg and 10 uL of resuspended glutathione magnetic agarose beads
435 (Pierce) in buffer A (125 mM Tris, 150 mM NaCl, 10 mM DTT, 1 mM EDTA, pH 7.4)
436 supplemented with 1X cOmplete protease inhibitor (EDTA-free, Roche). Samples were
437 incubated at 4°C for one hour. Beads were then washed four times with buffer A and proteins
438 were eluted with Laemmli sample buffer for analysis by western blotting. Antibodies used in
439 this study are described in Table S2.
440 For comparison of VPg pulldown by nCBP-2 variants across experiments, nCBP-2 and
441 VPg eluate band intensities were first measured using Image Lab (Bio-Rad). Within an
442 experiment, eluate VPg band intensities were first adjusted to correct for differing pulldown
443 efficiencies of each nCBP-2 variant using the following equation where VPg_X is VPg band
444 intensity for sample X and GST_X is full length GST fusion protein band intensity for sample X:

445 $$VPg_{X,\ adjusted} = VPg_X\ adjusted\ for\ GST\ fusion\ protein\ pulldown\ efficiency = \frac{VPg_X}{\left(\frac{GST_X}{GST_{nCBP-2}}\right)}$$

446 Adjusted VPg intensities were then expressed relative to the VPg intensity of the wild-type
447 nCBP-2 sample for that experiment:

448 $$Normalized\ VPg_X = \frac{VPg_{X,\ adjusted}}{VPg_{nCBP-2,\ adjusted}} \times 100$$

449

450 **Yeast two-hybrid assays**

451 All yeast two-hybrid experiments were performed using the EGY48 strain harboring
452 the pSH18-34 *lacZ* reporter plasmid along with pJG4-5 and pEG202 bait and prey plasmids
453 (Golemis & Khazak, 1997). pJG4-5 *CBSV VPg* bait plasmid and pEG202 *nCBP-2* prey
454 plasmids were created by using In-Fusion cloning (Takara) to insert CBSV VPg or nCBP-2
455 coding sequences into pJG4-5 or pEG202 linearized with EcoRI and XhoI. For qualitative
456 yeast two-hybrid experiments, EGY48 pSH18-34 yeast transformed with bait and prey
457 plasmids were first selected for on SD –ura –trp –his media supplemented with 2% glucose
458 (Gietz & Schiestl, 2007). Transformants were then plated onto SD –ura –trp –his media
459 supplemented with 2% galactose, 1% raffinose, 1X BU salts, and X-gal. Blue/white screening
460 was performed three to four days later. Quantitative yeast two-hybrid was performed using a
461 spectrophotometric β-galactosidase activity assay (Amberg *et al.*, 2006). To extract protein for
462 western blotting, 1 mL of yeast at OD600=2 was pelleted, resuspended in 0.1M NaOH,
463 incubated at room temperature for five minutes, pelleted, resuspended in Laemmli sample
464 buffer, incubated at 95C for five minutes, and pelleted again. The resulting supernatant was
465 used for SDS-PAGE and western blot analysis.

466 To screen for nCBP-2 mutants that lose affinity for CBSV VPg, pEG202 *nCBP-2* was
467 used as template for mutagenic PCR (Genemorph II, Agilent). Primers immediately flanking
468 the second and penultimate codon of *nCBP-2*, preserving the start and stop codons during
469 mutagenic PCR, were used with the low mutation rate protocol from the Genmorph II kit
470 (Agilent). pEG202 empty vector was then digested with EcoRI and SacI and the fragment
471 containing the yeast *HIS* marker was gel purified (Qiagen). A third pEG202 fragment
472 containing the yeast 2μ origin of replication was produced by PCR with ends that overlap the
473 *nCBP-2* mutant amplicons and pEG202 *HIS* marker fragment by 30 base pairs; co-
474 transformation of all three fragments into yeast result in assembly of an intact pEG202 *nCBP-*
475 *2* plasmid through yeast recombinational cloning. Mutant *nCBP-2* amplicons, pEG202 *HIS*
476 fragment, and pEG202 2μ fragment were mixed in a 4:1:1 molar ratio and co-transformed into
477 EGY48 yeast harboring the pSH18-34 and pJG4-5 *CBSV VPg* plasmids. Transformed yeast
478 were directly plated onto SD –ura –trp –his media supplemented with 2% galactose, 1%
479 raffinose, 1X BU salts, and X-gal. Four days post transformation, white or light blue colonies

480 were restreaked onto a new plate for further visual assessment of reduced β-galactosidase
481 activity. The yeast were then checked by PCR for the presence of full length *nCBP-2* insert in
482 pEG202 using vector backbone specific primers. *nCBP-2* mutant alleles were then amplified
483 from insert positive yeast using Q5 Hot Start polymerase (NEB) and analyzed by Sanger
484 sequencing.
485
486 **Yeast *eif4e* complementation assay**
487 3xFLAG and nCBP-2 or mutant nCBP-2 coding sequences were cloned into pG1.1
488 linearized with NcoI and BamHI using In-Fusion (Takara) to produce pG1.1 *3xFLAG-nCBP-2*.
489 *3xFLAG* was amplified from pB7-HFC (Huang *et al.*, 2016) while *nCBP-2* variants were
490 amplified from pEG202 yeast two-hybrid plasmids. pG1.1 plasmids were then transformed into
491 the conditional yeast *eif4e* mutant strain T93C (*eif4e*::LEU2 *ura3 trp1 leu2* [pGAL1-eIF4E
492 *URA3*]) (Altmann *et al.*, 1989). Transformants were plated on SD –ura –trp dropout media
493 containing 2% galactose and 1% raffinose and allowed to grow for five to seven days. Colonies
494 of transformed yeast were then resuspended in sterile water and a ten-fold dilution series
495 ranging from OD600 = 10^{-1} through 10^{-4} was plated on SD –ura –trp dropout media containing
496 2% glucose to examine for rescue by pG1.1 encoded *eIF4E*-family gene variants. Plates were
497 imaged after 5-7 days.
498
499 **SDS-PAGE and western blotting**
500 Proteins in Laemmli buffer were run on TruPAGE Triethanolamine-tricine (SIGMA,
501 discontinued) or Novex WedgeWell Tris-glycine (Thermo Fisher) SDS-PAGE gels according
502 to manufacturer's instructions. Samples were run alongside Benchmark Pre-stained or
503 PageRuler Prestained protein ladders (Thermo Scientific). We note that kDa markers were
504 observed to shift up to 15 kDa depending on gel and buffer chemistry. Proteins were then
505 transferred onto Immobilon-PSQ PVDF membranes (Sigma) at 100V constant for one hour.
506 After blocking in 5% milk in TBST, proteins were detected by probing with antibodies listed in
507 Table S2. After imaging, membranes were immediately rinsed in TBST and stained with
508 Coomassie R250 to check for equal loading.
509
510 **Acknowledgements**
511 We would like to thank the DDPSC PGF team for their hard work in caring for our
512 plants. We thank Claire Albin for her assistance with CBSV challenges and Nigel Taylor for
513 allowing us to use Taylor Lab greenhouse space. Yeast strain T93C, pG1.1 At_eIF4E1, and
514 pG1.1 empty vector were generously provided by Dr. Karen S. Browning. Z.D.L. would like to
515 thank Susan Lin, Wei-Yang Lin, Chun-Hwa Lin, and Jocelyn Lin for their love and support.
516 Z.D.L. was funded by USDA NIFA award 2019-67012-29626 and the Bill & Melinda Gates

517 Foundation (OPP1125410, R.B.S., S.E.J., J.C.C.). E.J.D., Z.V.B., H.T., E.H., and A.M. were
518 funded by the DDPSC NSF-REU program, DBI-1659812, -2050394, -1659812, and -2244275.
519

520 **Competing Interests**

521 None to declare.

522

523 **Author Contributions**

524 Conceptualization: Z.D.L.; Methodology: Z.D.L., J.C.C., R.S.B.; Investigation: Z.D.L.,
525 M.K.S., G.L.H., E.D.M., Z.V.B., K.B., H.T., E.H., G.J., K.B.G.; Visualization: Z.D.L.; Writing –
526 original draft: Z.D.L.; Writing – reviewing & editing: Z.D.L., K.B.G., J.C.C., R.S.B.

527

528 **Data Availability**

529 The source data for all results presented in this study are provided in accompanying
530 supplementary files.

531

532 **References**

533 ***Agricultural production statistics 2000–2022***. **2023**. Rome, Italy: Food & Agriculture
534 Organization of the United Nations (FAO).

535 **Altmann M**, **Sonenberg N**, **Trachsel H**. **1989**. Translation in Saccharomyces cerevisiae:
536 initiation factor 4E-dependent cell-free system. *Molecular and cellular biology* **9**: 4467–4472.

537 **Amberg DC**, **Burke DJ**, **Strathern JN**. **2006**. Assay of β-galactosidase in yeast:
538 Permeabilized cell assay. *CSH protocols* **2006**: db.prot4158.

539 **Ashby JA**, **Stevenson CEM**, **Jarvis GE**, **Lawson DM**, **Maule AJ**. **2011**. Structure-based
540 mutational analysis of eIF4E in relation to sbm1 resistance to pea seed-borne mosaic virus
541 in pea. *PloS one* **6**: e15873.

542 **Bae S**, **Park J**, **Kim J-S**. **2014**. Cas-OFFinder: a fast and versatile algorithm that searches
543 for potential off-target sites of Cas9 RNA-guided endonucleases. *Bioinformatics (Oxford,*
544 *England)* **30**: 1473–1475.

545 **Bastet A**, **Lederer B**, **Giovinazzo N**, **Arnoux X**, **German-Retana S**, **Reinbold C**, **Brault V**,
546 **Garcia D**, **Djennane S**, **Gersch S**, *et al.* **2018**. Trans-species synthetic gene design allows
547 resistance pyramiding and broad-spectrum engineering of virus resistance in plants. *Plant*
548 *biotechnology journal* **16**: 1569–1581.

549 **Bastet A**, **Robaglia C**, **Gallois J-L**. **2017**. EIF4E resistance: Natural variation should guide

550 gene editing. *Trends in plant science* **22**: 411–419.

551 **Bastet A**, **Zafirov D**, **Giovinazzo N**, **Guyon-Debast A**, **Nogué F**, **Robaglia C**, **Gallois J-L**.
552 **2019**. Mimicking natural polymorphism in eIF4E by CRISPR-Cas9 base editing is associated
553 with resistance to potyviruses. *Plant biotechnology journal* **17**: 1736–1750.

554 **Beyene G**, **Chauhan RD**, **Ilyas M**, **Wagaba H**, **Fauquet CM**, **Miano D**, **Alicai T**, **Taylor NJ**.
555 **2016**. A virus-derived stacked RNAi construct confers robust resistance to cassava brown
556 streak disease. *Frontiers in plant science* **7**: 2052.

557 **Bredeson JV**, **Lyons JB**, **Prochnik SE**, **Wu GA**, **Ha CM**, **Edsinger-Gonzales E**,
558 **Grimwood J**, **Schmutz J**, **Rabbi IY**, **Egesi C**, *et al.* **2016**. Sequencing wild and cultivated
559 cassava and related species reveals extensive interspecific hybridization and genetic
560 diversity. *Nature biotechnology* **34**: 562–570.

561 **Browning KS**, **Bailey-Serres J**. **2015**. Mechanism of cytoplasmic mRNA translation. *The*
562 *Arabidopsis book* **13**: e0176.

563 **Čermák T**, **Curtin SJ**, **Gil-Humanes J**, **Čegan R**, **Kono TJY**, **Konečná E**, **Belanto JJ**,
564 **Starker CG**, **Mathre JW**, **Greenstein RL**, *et al.* **2017**. A multipurpose toolkit to enable
565 advanced genome engineering in plants. *The plant cell* **29**: 1196–1217.

566 **Charron C**, **Nicolaï M**, **Gallois J-L**, **Robaglia C**, **Moury B**, **Palloix A**, **Caranta C**. **2008**.
567 Natural variation and functional analyses provide evidence for co-evolution between plant
568 eIF4E and potyviral VPg. *The Plant journal: for cell and molecular biology* **54**: 56–68.

569 **Concordet J-P**, **Haeussler M**. **2018**. CRISPOR: intuitive guide selection for CRISPR/Cas9
570 genome editing experiments and screens. *Nucleic acids research* **46**: W242–W245.

571 **Connelly JP**, **Pruett-Miller SM**. **2019**. CRIS.Py: A versatile and high-throughput analysis
572 program for CRISPR-based genome editing. *Scientific reports* **9**: 4194.

573 **Coutinho de Oliveira L**, **Volpon L**, **Rahardjo AK**, **Osborne MJ**, **Culjkovic-Kraljacic B**,
574 **Trahan C**, **Oeffinger M**, **Kwok BH**, **Borden KLB**. **2019**. Structural studies of the eIF4E-VPg
575 complex reveal a direct competition for capped RNA: Implications for translation.
576 *Proceedings of the National Academy of Sciences of the United States of America* **116**:
577 24056–24065.

578 **Dombrovsky A**, **Reingold V**, **Antignus Y**. **2014**. Ipomovirus--an atypical genus in the family
579 Potyviridae transmitted by whiteflies. *Pest management science* **70**: 1553–1567.

580 **Duprat A**, **Caranta C**, **Revers F**, **Menand B**, **Browning KS**, **Robaglia C**. **2002**. The
581 Arabidopsis eukaryotic initiation factor (iso)4E is dispensable for plant growth but required
582 for susceptibility to potyviruses. *The Plant journal: for cell and molecular biology* **32**: 927–
583 934.

584 **Gallois J-L**, **Charron C**, **Sánchez F**, **Pagny G**, **Houvenaghel M-C**, **Moretti A**, **Ponz F**,
585 **Revers F**, **Caranta C**, **German-Retana S**. **2010**. Single amino acid changes in the turnip
586 mosaic virus viral genome-linked protein (VPg) confer virulence towards Arabidopsis
587 thaliana mutants knocked out for eukaryotic initiation factors eIF(iso)4E and eIF(iso)4G. *The*
588 *Journal of general virology* **91**: 288–293.

589 **Gao L**, **Luo J**, **Ding X**, **Wang T**, **Hu T**, **Song P**, **Zhai R**, **Zhang H**, **Zhang K**, **Li K**, *et al.*
590 **2020**. Soybean RNA interference lines silenced for eIF4E show broad potyvirus resistance.
591 *Molecular plant pathology* **21**: 303–317.

592 **Gauffier C**, **Lebaron C**, **Moretti A**, **Constant C**, **Moquet F**, **Bonnet G**, **Caranta C**, **Gallois**
593 **J-L**. **2016**. A TILLING approach to generate broad-spectrum resistance to potyviruses in
594 tomato is hampered by eIF4E gene redundancy. *The Plant journal: for cell and molecular*
595 *biology* **85**: 717–729.

596 **German-Retana S**, **Walter J**, **Doublet B**, **Roudet-Tavert G**, **Nicaise V**, **Lecampion C**,
597 **Houvenaghel M-C**, **Robaglia C**, **Michon T**, **Le Gall O**. **2008**. Mutational analysis of plant
598 cap-binding protein eIF4E reveals key amino acids involved in biochemical functions and
599 potyvirus infection. *Journal of virology* **82**: 7601–7612.

600 **Gietz RD**, **Schiestl RH**. **2007**. Frozen competent yeast cells that can be transformed with
601 high efficiency using the LiAc/SS carrier DNA/PEG method. *Nature protocols* **2**: 1–4.

602 **Golemis EA**, **Khazak V**. **1997**. Alternative yeast two-hybrid systems. The interaction trap
603 and interaction mating. *Methods in molecular biology (Clifton, N.J.)* **63**: 197–218.

604 **Gomez MA**, **Lin ZD**, **Moll T**, **Chauhan RD**, **Hayden L**, **Renninger K**, **Beyene G**, **Taylor NJ**,
605 **Carrington JC**, **Staskawicz BJ**, *et al.* **2019**. Simultaneous CRISPR/Cas9-mediated editing
606 of cassava eIF4E isoforms nCBP-1 and nCBP-2 reduces cassava brown streak disease
607 symptom severity and incidence. *Plant biotechnology journal* **17**: 421–434.

608 **Grüner S**, **Peter D**, **Weber R**, **Wohlbold L**, **Chung M-Y**, **Weichenrieder O**, **Valkov E**,
609 **Igreja C**, **Izaurralde E**. **2016**. The structures of eIF4E-eIF4G complexes reveal an extended
610 interface to regulate translation initiation. *Molecular cell* **64**: 467–479.

611 **Grüner S**, **Weber R**, **Peter D**, **Chung M-Y**, **Igreja C**, **Valkov E**, **Izaurralde E**. **2018**.
612 Structural motifs in eIF4G and 4E-BPs modulate their binding to eIF4E to regulate translation
613 initiation in yeast. *Nucleic acids research* **46**: 6893–6908.

614 **Hart JP**, **Griffiths PD**. **2013**. A series of eIF4E alleles at the Bc-3 locus are associated with
615 recessive resistance to Clover yellow vein virus in common bean. *Theoretical and applied*
616 *genetics* **126**: 2849–2863.

617 **Huang H**, **Alvarez S**, **Bindbeutel R**, **Shen Z**, **Naldrett MJ**, **Evans BS**, **Briggs SP**, **Hicks**
618 **LM**, **Kay SA**, **Nusinow DA**. **2016**. Identification of evening complex associated proteins in
619 Arabidopsis by affinity purification and mass spectrometry. *Molecular & cellular proteomics:*
620 *MCP* **15**: 201–217.

621 **Kang B-C**, **Yeam I**, **Frantz JD**, **Murphy JF**, **Jahn MM**. **2005**. The pvr1 locus in Capsicum
622 encodes a translation initiation factor eIF4E that interacts with Tobacco etch virus VPg. *The*
623 *Plant journal: for cell and molecular biology* **42**: 392–405.

624 **Kelley LA**, **Mezulis S**, **Yates CM**, **Wass MN**, **Sternberg MJE**. **2015**. The Phyre2 web portal
625 for protein modeling, prediction and analysis. *Nature protocols* **10**: 845–858.

626 **Kim J**, **Kang W-H**, **Hwang J**, **Yang H-B**, **Dosun K**, **Oh C-S**, **Kang B-C**. **2014**. Transgenic
627 Brassica rapa plants over-expressing eIF(iso)4E variants show broad-spectrum Turnip
628 mosaic virus (TuMV) resistance. *Molecular plant pathology* **15**: 615–626.

629 **Lebaron C**, **Rosado A**, **Sauvage C**, **Gauffier C**, **German-Retana S**, **Moury B**, **Gallois J-L**.
630 **2016**. A new eIF4E1 allele characterized by RNAseq data mining is associated with
631 resistance to potato virus Y in tomato albeit with a low durability. *The Journal of general*
632 *virology* **97**: 3063–3072.

633 **Léonard S**, **Plante D**, **Wittmann S**, **Daigneault N**, **Fortin MG**, **Laliberté JF**. **2000**. Complex
634 formation between potyvirus VPg and translation eukaryotic initiation factor 4E correlates
635 with virus infectivity. *Journal of virology* **74**: 7730–7737.

636 **Li H**, **Kondo H**, **Kühne T**, **Shirako Y**. **2016**. Barley yellow mosaic virus VPg is the
637 determinant protein for breaking eIF4E-mediated recessive resistance in barley plants.
638 *Frontiers in plant science* **7**: 1449.

639 **Madeira F, Madhusoodanan N, Lee J, Eusebi A, Niewielska A, Tivey ARN, Lopez R,**
640 **Butcher S. 2024**. The EMBL-EBI Job Dispatcher sequence analysis tools framework in
641 2024. Nucleic acids research **52**: W521–W525.

642 **Miyoshi H**, **Suehiro N**, **Tomoo K**, **Muto S**, **Takahashi T**, **Tsukamoto T**, **Ohmori T**,
643 **Natsuaki T**. **2006**. Binding analyses for the interaction between plant virus genome-linked
644 protein (VPg) and plant translational initiation factors. *Biochimie* **88**: 329–340.

645 **Naderpour M**, **Lund OS**, **Larsen R**, **Johansen E**. **2010**. Potyviral resistance derived from
646 cultivars of Phaseolus vulgaris carrying bc-3 is associated with the homozygotic presence of
647 a mutated eIF4E allele. *Molecular plant pathology* **11**: 255–263.

648 **Odipio J**, **Ogwok E**, **Taylor NJ**, **Halsey M**, **Bua A**, **Fauquet CM**, **Alicai T**. **2014**. RNAi-
649 derived field resistance to Cassava brown streak disease persists across the vegetative
650 cropping cycle. *GM crops & food* **5**: 16–19.

651 **Revers F**, **García JA**. **2015**. Molecular biology of potyviruses. *Advances in virus research*
652 **92**: 101–199.

653 **Rey C**, **Vanderschuren H**. **2017**. Cassava mosaic and brown streak diseases: Current
654 perspectives and beyond. *Annual review of virology* **4**: 429–452.

655 **Robaglia C**, **Caranta C**. **2006**. Translation initiation factors: a weak link in plant RNA virus
656 infection. *Trends in plant science* **11**: 40–45.

657 **Robson F**, **Hird DL**, **Boa E**. **2023**. Cassava brown streak: A deadly virus on the move. *Plant*
658 *pathology*.

659 **Sanfaçon H**. **2015**. Plant translation factors and virus resistance. *Viruses* **7**: 3392–3419.

660 **Schaad MC**, **Anderberg RJ**, **Carrington JC**. **2000**. Strain-specific interaction of the tobacco
661 etch virus NIa protein with the translation initiation factor eIF4E in the yeast two-hybrid
662 system. *Virology* **273**: 300–306.

663 **Sheat S**, **Winter S**. **2023**. Developing broad-spectrum resistance in cassava against viruses
664 causing the cassava mosaic and the cassava brown streak diseases. *Frontiers in plant*
665 *science* **14**: 1042701.

666 **Takakura Y**, **Udagawa H**, **Shinjo A**, **Koga K**. **2018**. Mutation of a Nicotiana tabacum L.
667 eukaryotic translation-initiation factor gene reduces susceptibility to a resistance-breaking
668 strain of Potato virus Y. *Molecular plant pathology* **19**: 2124–2133.

669 **Taylor N**, **Gaitán-Solís E**, **Moll T**, **Trauterman B**, **Jones T**, **Pranjal A**, **Trembley C**,
670 **Abernathy V**, **Corbin D**, **Fauquet CM**. **2012**. A high-throughput platform for the production
671 and analysis of transgenic cassava (Manihot esculenta) plants. *Tropical plant biology* **5**:

127–139.

Tomlinson KR, **Bailey AM**, **Alicai T**, **Seal S**, **Foster GD**. **2018**. Cassava brown streak disease: historical timeline, current knowledge and future prospects. *Molecular plant pathology* **19**: 1282–1294.

Upadhyay V, Lucas A, Patrick C, Mallela KMG. 2024. Isothermal titration calorimetry and surface plasmon resonance methods to probe protein-protein interactions. Methods (San Diego, Calif.) **225**: 52–61.

Valli A, **García JA**, **López-Moya JJ**. **2015**. Potyviridae. *Encyclopedia of Life Sciences*: 1–10.

Veley KM, **Elliott K**, **Jensen G**, **Zhong Z**, **Feng S**, **Yoder M**, **Gilbert KB**, **Berry JC**, **Lin Z-JD**, **Ghoshal B**, *et al.* **2023**. Improving cassava bacterial blight resistance by editing the epigenome. *Nature communications* **14**: 85.

Wagaba H, Beyene G, Trembley C, Alicai T, Fauquet CM, Taylor NJ. 2013. Efficient transmission of cassava brown streak disease viral pathogens by chip bud grafting. BMC research notes **6**: 516.

Wagaba H, **Beyene G**, **Aleu J**, **Odipio J**, **Okao-Okuja G**, **Chauhan RD**, **Munga T**, **Obiero H**, **Halsey ME**, **Ilyas M**, *et al.* **2016**. Field level RNAi-mediated resistance to cassava brown streak disease across multiple cropping cycles and diverse East African Agro-ecological locations. *Frontiers in plant science* **7**: 2060.

Walker PJ, **Siddell SG**, **Lefkowitz EJ**, **Mushegian AR**, **Adriaenssens EM**, **Alfenas-Zerbini P**, **Dempsey DM**, **Dutilh BE**, **García ML**, **Curtis Hendrickson R**, *et al.* **2022**. Recent changes to virus taxonomy ratified by the International Committee on Taxonomy of Viruses (2022). *Archives of virology* **167**: 2429–2440.

Wittmann S, **Chatel H**, **Fortin MG**, **Laliberté JF**. **1997**. Interaction of the viral protein genome linked of turnip mosaic potyvirus with the translational eukaryotic initiation factor (iso) 4E of Arabidopsis thaliana using the yeast two-hybrid system. *Virology* **234**: 84–92.

Yang X, **Li Y**, **Wang A**. **2021**. Research advances in potyviruses: From the laboratory bench to the field. *Annual review of phytopathology* **59**: 1–29.

Yeam I, **Cavatorta JR**, **Ripoll DR**, **Kang B-C**, **Jahn MM**. **2007**. Functional dissection of naturally occurring amino acid substitutions in eIF4E that confers recessive potyvirus resistance in plants. *The plant cell* **19**: 2913–2928.

703 **Zafirov D**, **Giovinazzo N**, **Bastet A**, **Gallois J-L**. **2021**. When a knockout is an Achilles'
704 heel: Resistance to one potyvirus species triggers hypersusceptibility to another one in
705 Arabidopsis thaliana. *Molecular plant pathology* **22**: 334–347.

706 **Supporting Information**

707 **Fig. S1** Wild type aerial and storage root disease scores across all challenges
708 **Fig. S2** gRNAs used in this study
709 **Fig. S3** *eIF4E*-family mutant cassava plants
710 **Fig. S4** Representative *eif(iso)4e-1 eif(iso)4e-2* double mutant and wild type TME419 six
711 weeks post transfer to soil
712 **Fig. S5** Storage root photos of CBSV infected mutant cassava
713 **Fig. S6** Purified proteins for GST pulldown assays
714 **Fig. S7** Alignment of ipomovirus and potyvirus VPg's show significant divergence in AA
715 sequences
716 **Fig. S8** Alignment of cassava eIF4E-family proteins
717 **Fig. S9** Quantitative yeast two-hybrid assay confirms loss-of-affinity screen results
718 **Fig. S10** Western blot analysis of yeast strains used for yeast two-hybrid experiments
719 **Fig. S11** Accumulation of eIF4E-family proteins and CBSV VPg in yeast used for quantitative
720 yeast two-hybrid analysis
721 **Fig. S12** Effects of mutating the HPL motif leucine in *Arabidopsis* eIF(iso)4E
722 **Table S1** TME419 gRNA off-target sites
723 **Table S2** Antibodies used in this study
724 **Table S3** Gene editing outcomes for TME419 eIF4E-family mutants
725 **Table S4** All nCBP-2 loss-of-VPg-affinity mutants identified by yeast two-hybrid
726

727 **Figure legends**

728 **Fig. 1 Endpoint CBSD storage root disease severity in cassava eIF4E-family mutants**
729 a, b) Endpoint aerial disease (a) and storage root necrosis (b) observed in cassava eIF4E-
730 family single and double mutants after challenge with CBSV isolate Naliendele. Data
731 presented are an aggregate from all experimental replicates. Leaf and stem disease
732 symptoms are evaluated separately on a 0-5 scale and then added together for a total aerial
733 symptom score. Storage root necrosis severity was scored on a 1 to 5 scale, 1 being
734 asymptomatic and 5 corresponding to severe necrosis throughout all storage roots of a
735 plant. Mann-Whitney U test was used to detect statistical differences with an alpha = 0.05. *
736 ≤ 0.05, ** ≤ 0.01, *** ≤ 0.001. Asterisks above boxplots denote differences from wild type,
737 while asterisks above brackets indicate differences between indicated genotypes.

738 c) qRT-PCR quantification of storage root CBSV viral levels from challenged mutants. CBSV
739 HAM1 was quantified relative to cassava PP2A to obtain HAM1 normalized relative
740 quantities (NRQs). HAM1 NRQs for each genotype are presented as relative to the mean of
741 wild type. Statistical differences were detected with the Mann-Whitney U test as described in
742 (a, b).
743 d) Representative storage root sections from wild type and ncbp-1 ncbp-2 #213 plants
744 challenged with CBSV. Scale bar denotes 1 cm.

745 **Figure 2. Interaction of GST-cassava eIF4E family proteins and CBSV VPg *in vitro***
746 a, b) GST-pulldown assays were performed with CBSV VPg-6xHis-3xFLAG and GST or
747 GST-tagged cassava eIF4E-family proteins. Proteins were expressed in and purified from *E.*
748 *coli*. Human (Hs) eIF4E was also tested in (a).
749 c) Model for eIF4E-mediated resistance against potyvirids. Cartoon depicts potyvirid
750 genome-linked VPg protein bound to eIF4E-family protein in order to cause disease, while
751 mutations that disrupt this interaction results in resistance.
752 d) Coimmunoprecipitation of YFP or YFP- eIF4E-family proteins with TuMV 6xHis-VPg-
753 6xHIS-3xFLAG. VPg was expressed in and purified from *E. coli* and then mixed with extract
754 from *N. benthamiana* leaves expressing YFP or YFP-fusion proteins.
755 e) *Arabidopsis* eIF(iso)4E residues 92 through 150 aligned with homologous regions of
756 cassava eIF4E-family proteins. W92 and K150, marked red, are necessary for interaction
757 with TuMV VPg. * indicates conservation across all aligned proteins, : indicates conservation
758 of amino acids with strongly similar properties, and . indicates conservation of amino acids
759 with weakly similar properties.
760 f) GST-pulldown assay as in a) and b) with CBSV VPg incubated with either GST, GST-
761 nCBP-2, and GST-nCBP-2$^{W118L/N170E}$.
762 g) Comparison of nCBP-2 and nCBP-2$^{W118L/N170E}$ interaction with CBSV VPg by quantitative
763 yeast two-hybrid assay.
764 h) Western blot analysis of nCBP-2 and VPg expression in yeast from g).

765 **Fig. 3 A yeast two-hybrid loss-of-affinity screen identifies nCBP-2 residues necessary**
766 **for VPg interaction**
767 a) Workflow for using a yeast two-hybrid approach to identify nCBP-2 mutants that lose
768 affinity for CBSV Naliendele VPg. The resultant pEG202 prey vector encodes nCBP-2 fused
769 to the LexA DNA binding domain. pJG4-5 encodes CBSV VPg fused to the B42
770 transcriptional activation domain. The EGY48 yeast strain used harbors the pSH18-34
771 reporter plasmid containing *lacZ* driven by the LexA operator.
772 b) Ventral and dorsal views of cassava nCBP-2 structure produced using the Phyre2 server

773 (Kelley *et al.*, 2015). nCBP-2 structure of amino acids 49 through 226 was predicted using
774 wheat eIF4E (PDB ID: 2IDR) as a template. Mutated amino acid residues in nCBP-2 mutants
775 that lose VPg affinity and either rescue or fail to rescue *eif4e* yeast are highlighted in green
776 and pink, respectively. W118 and N170, homologous with TuMV VPg interacting residues of
777 *Arabidopsis* eIF(iso)4E, are highlighted in blue.

778 **Fig. 4 T93C *eif4e* yeast complementation by *nCBP-2* mutants**
779 a) Schematic for testing translation initiation activity of *nCBP-2* variants expressed from the
780 pG1.1 plasmid in T93C *eif4e* conditional mutant yeast.
781 b) Left panels: T93C yeast transformed with pG1.1 empty vector or pG1.1 encoding various
782 eIF4E-proteins grown on SD dropout media supplemented with galactose allowing for
783 conditional expression of yeast eIF4E from the pGAL1-eIF4E plasmid. Right panels: same
784 yeast strains from left panel grown on dropout media supplemented with glucose, preventing
785 complementation by the pGAL1-eIF4E plasmid.
786 c) Western blot analysis of 3xFLAG tagged nCBP-2 variant expression in yeast strains used
787 in a). Coomassie stained membrane is presented for assessing loading control.

788 **Fig. 5 Effects of HPL motif mutation on nCBP-2 affinity for CBSV VPg and translation**
789 **initiation**
790 a) Alignment of human eIF4E protein sequence with variants of cassava nCBP-2. The
791 conserved HPL motif is boxed in red and the L51F mutation in nCBP-2 is highlighted in cyan.
792 Asterisks denote conserved amino acid residues.
793 b) Quantitative yeast two-hybrid analysis of CBSV VPg interaction with nCBP-2 variants.
794 c) T93C *eif4e* yeast transformed with pG1.1 encoding *Arabidopsis eIF4E1* or cassava *nCBP-*
795 *2* variants under the control of a constitutive promoter. nCBP-2 variants are N-terminally
796 tagged with 3xFLAG. The T93C yeast strain harbors a plasmid encoding galactose-inducible
797 and glucose-repressible yeast *eIF4E*.
798 d) Western blot analysis of nCBP-2 expression in yeast used in c). A segment of coomassie
799 stained membrane is presented for loading control.

800 **Fig. 6 nCBP-2^{K45_L51del} and nCBP-2^{L51F} exhibit reduced affinity for CBSV VPg, *in vitro***
801 a) GST pulldown experiment assessing the ability of GST-nCBP-2 variants to bind CBSV
802 VPg. Full-length protein eluate band intensities are presented underneath the eluate western
803 blots and are expressed relative to the sample with the strongest band intensity.
804 b) Analysis of eluate VPg band intensity across three GST-pulldown experiments. Band
805 intensities are normalized to account for differing amounts of GST-fusion protein pulled down
806 and expressed relative to VPg intensity in the GST-nCBP-2 sample.

807 **Fig. 7 Effects of mutating the HPL motif leucine in cassava *eIF4E* and *eIF(iso)4E***
808 a, b) Quantitative yeast two-hybrid analysis of CBSV VPg interaction with wild type cassava
809 eIF4E-famiy proteins alongside HPL to HPF mutants. Assays were performed after growing
810 yeast under VPg inducing conditions for 48 hours. Results for eIF(iso)4E-1 and -2 interaction
811 with CBSV VPg in panel a), highlighted with a red box, are enlarged in panel b). Statistical
812 differences were detected using a Welch's T-test with an alpha = 0.05. ** ≤ 0.01, *** ≤ 0.001.
813 c) T93C *eif4e* yeast complementation assay with wild-type and mutant *eIF4E*-family genes
814 from cassava

815

816

817

818

819

820

821

822

823

824

825

826

827

828

829

830

831

832

Table 1. TME419 CRISPR mutant genotypes

Line #	CRISPR target	Gene/allele	INDEL	Protein nomenclature
6-95	*eIF4E*	*A*	-2	S21*fsX1
		B	–	"
172	*iso4E1+2*	*iso4E1 A*	-1	A11PfsX17
		iso4E1 B	-2	A11HfsX9
		iso4E2 A	-2	I7RfsX29
		iso4E2 B	1	E8RfsX36
92	*iso4E1+2*	*iso4E1 A*	-2	A11HfsX9
		iso4E1 B	-1	A11PfsX17
		iso4E2 A	-2	I7RfsX29
		iso4E2 B	1	E8RfsX36
10-9	*iso4E2*	*A*	1	E8RfsX36
		B	–	"
3-29	*iso4E1*	*A*	-1	A11PfsX17
		B	–	"
93	*nCBP1*	*A*	1	S23YfsX4
		B	-2	S23TfsX3
4-53	*nCBP2*	*A*	1	T23NfsX8
		B	–	"
213	*nCBP1+2*	*nCBP1 A*	1	S23YfsX4
		nCBP1 B	–	"
		nCBP2 A	-4	T22HfsX10
		nCBP2 B	-2	T23IfsX7
40	*nCBP1+2*	*nCBP1 A*	1	S23YfsX4
		nCBP1 B	1	P24TfsX3
		nCBP2 A	-21	K45_L51del
		nCBP2 B	-1	A46LfsX31

833

834

835

836

837

838

Table 2. Summary of nCBP-2 mutants found to lose affinity for CBSV VPg

No. loss-of-affinity mutants	Nucleotide substitutions per mutant (mean)	Nucleotide deletions per mutant (mean)	Unique alleles	No. unique AA substitutions	Frameshift mutants (unique/total)	Stop-gain mutants	Redundant AA substitution occurrences	AA residues with multiple occurrences of substitutions
51	1.37	0.15	46	48 [a]	7/8	7	7	8

[a] non-synonymous mutations downstream of frameshifting INDELs or stop-gain mutations are not counted

839

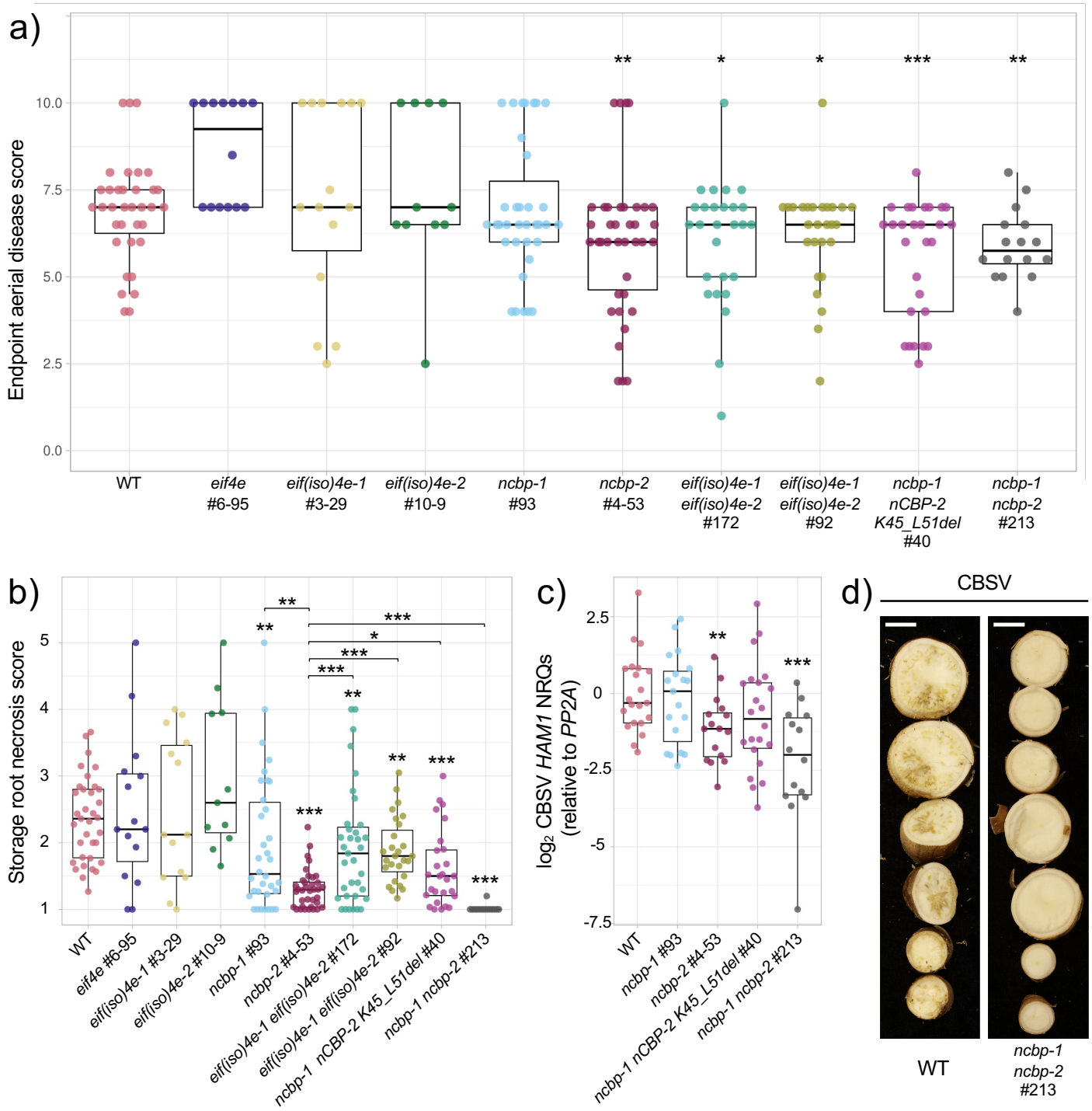

Fig. 1 Endpoint CBSD storage root disease severity in cassava *eIF4E*-family mutants

a, b) Endpoint aerial disease (a) and storage root necrosis (b) observed in cassava *eIF4E*-family single and double mutants after challenge with CBSV isolate Naliendele. Data presented are an aggregate from all experimental replicates. Leaf and stem disease symptoms are evaluated separately on a 0-5 scale and then added together for a total aerial symptom score. Storage root necrosis severity was scored on a 1 to 5 scale, 1 being asymptomatic and 5 corresponding to severe necrosis throughout all storage roots of a plant. Mann-Whitney U test was used to detect statistical differences with an alpha = 0.05. * ≤ 0.05, ** ≤ 0.01, *** ≤ 0.001. Asterisks above boxplots denote differences from wild type, while asterisks above brackets indicate differences between indicated genotypes.
c) qRT-PCR quantification of storage root CBSV viral levels from challenged mutants. CBSV *HAM1* was quantified relative to cassava *PP2A* to obtain *HAM1* normalized relative quantities (NRQs). *HAM1* NRQs for each genotype are presented as relative to the mean of wild type. Statistical differences were detected with the Mann-Whitney U test as described in (a, b).
d) Representative storage root sections from wild type and *ncbp-1 ncbp-2* #213 plants challenged with CBSV. Scale bar denotes 1 cm.

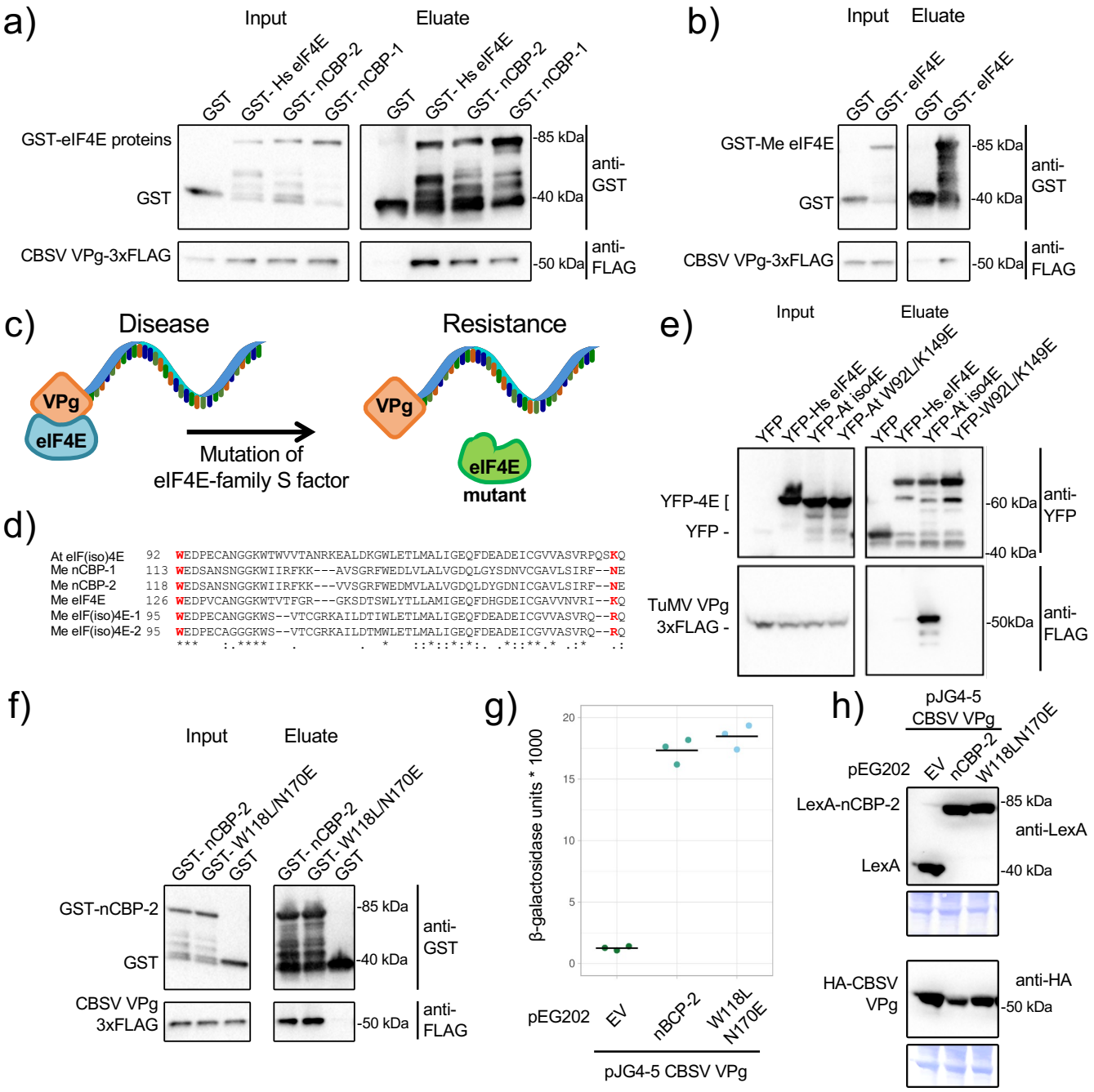

Figure 2. Interaction of GST-cassava eIF4E family proteins and CBSV VPg *in vitro*

a, b) GST-pulldown assays were performed with CBSV VPg-6xHis-3xFLAG and GST or GST-tagged cassava eIF4E-family proteins. Proteins were expressed in and purified from *E. coli*. Human (Hs) eIF4E was also tested in (a). Proteins were run on TEO-Tricine SDS-PAGE gels.
c) Model for eIF4E-mediated resistance against potyvirids. Cartoon depicts potyvirid genome-linked VPg protein bound to eIF4E-family protein in order to cause disease, while mutations that disrupt this interaction results in resistance.
d) Coimmunoprecipitation of YFP or YFP- eIF4E-family proteins with TuMV 6xHis-VPg-6xHIS-3xFLAG. VPg was expressed in and purified from *E. coli* and then mixed with extract from *N. benthamiana* leaves expressing YFP or YFP-fusion proteins.
e) *Arabidopsis* eIF(iso)4E residues 92 through 150 aligned with homologous regions of cassava eIF4E-family proteins. W92 and K150, marked red, are necessary for interaction with TuMV VPg. * indicates conservation across all aligned proteins, : indicates conservation of amino acids with strongly similar properties, and . indicates conservation of amino acids with weakly similar properties.
f) GST-pulldown assay as in a) and b) with CBSV VPg incubated with either GST, GST-nCBP-2, and GST-nCBP-2$^{W118L/N170E}$.
g) Comparison of nCBP-2 and nCBP-2$^{W118L/N170E}$ interaction with CBSV VPg by quantitative yeast two-hybrid assay.
h) Western blot analysis of nCBP-2 and VPg expression in yeast from g).

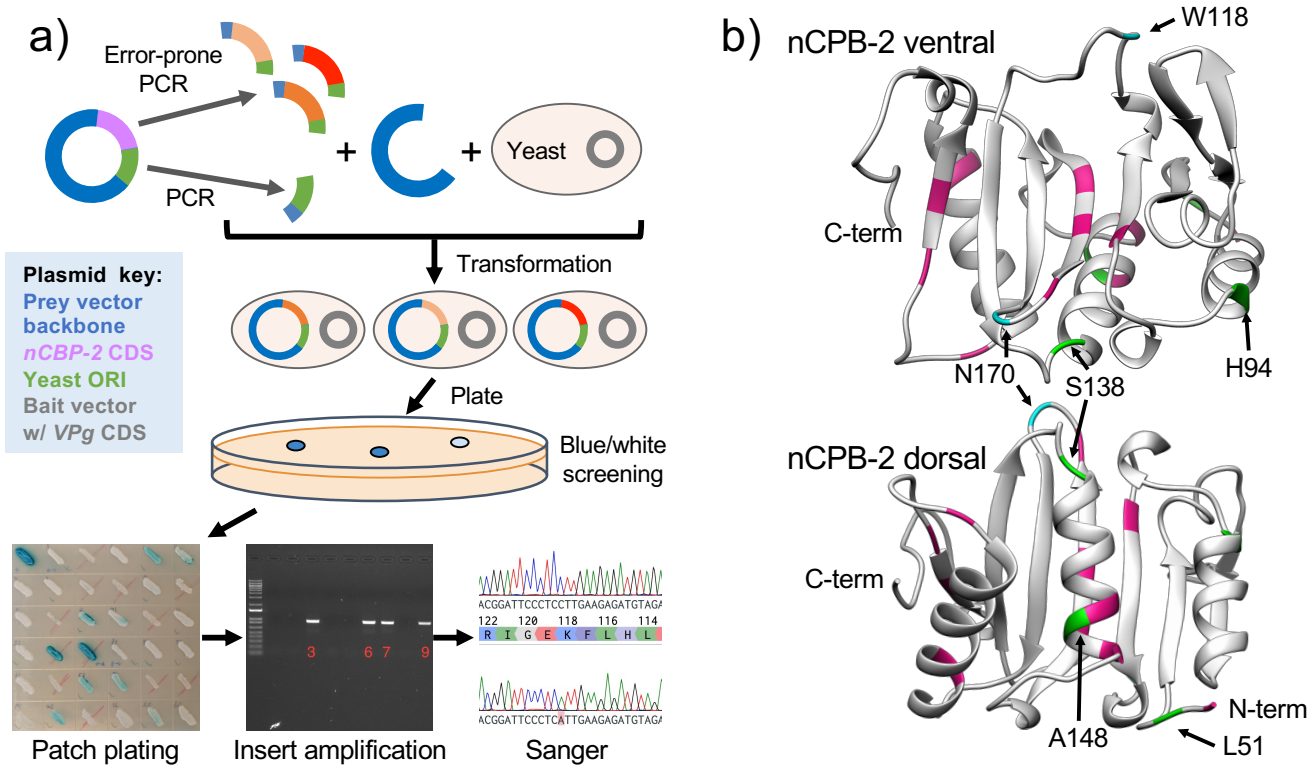

Fig. 3 A yeast two-hybrid loss-of-affinity screen identifies nCBP-2 residues necessary for VPg interaction

a) Workflow for using a yeast two-hybrid approach to identify nCBP-2 mutants that lose affinity for CBSV Naliendele VPg. The resultant pEG202 prey vector encodes nCBP-2 fused to the LexA DNA binding domain. pJG4-5 encodes CBSV VPg fused to the B42 transcriptional activation domain. The EGY48 yeast strain used harbors the pSH18-34 reporter plasmid containing *lacZ* driven by the LexA operator.
b) Ventral and dorsal views of cassava nCBP-2 structure produced using the Phyre2 server (Kelley LA et al., 2015). nCBP-2 structure of amino acids 49 through 226 was predicted using wheat eIF4E (PDB ID: 2IDR) as a template. Mutated amino acid residues in nCBP-2 mutants that lose VPg affinity and either rescue or fail to rescue *eif4e* yeast are highlighted in green and pink, respectively. W118 and N170, homologous with TuMV VPg interacting residues of *Arabidopsis* eIF(iso)4E, are highlighted in blue.

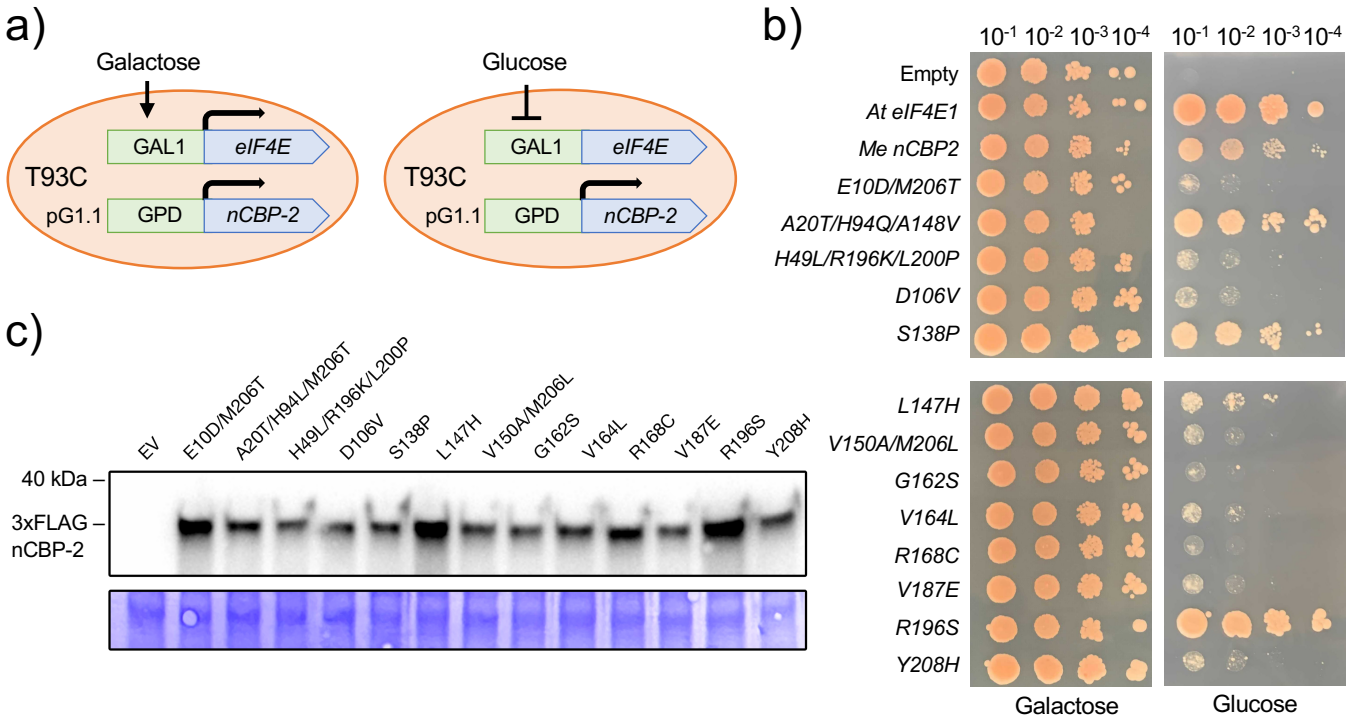

Fig. 4 T93C *eif4e* yeast complementation by *nCBP-2* mutants

a) Schematic for testing translation initiation activity of *nCBP-2* variants expressed from the pG1.1 plasmid in T93C *eif4e* conditional mutant yeast.
b) Left panels: T93C yeast transformed with pG1.1 empty vector or pG1.1 encoding various eIF4E-proteins grown on SD dropout media supplemented with galactose allowing for conditional expression of yeast eIF4E from the pGAL1-eIF4E plasmid. Right panels: same yeast strains from left panel grown on dropout media supplemented with glucose, preventing complementation by the pGAL1-eIF4E plasmid.
c) Western blot analysis of 3xFLAG tagged nCBP-2 variant expression in yeast strains used in a). Coomassie stained membrane is presented for assessing loading control.

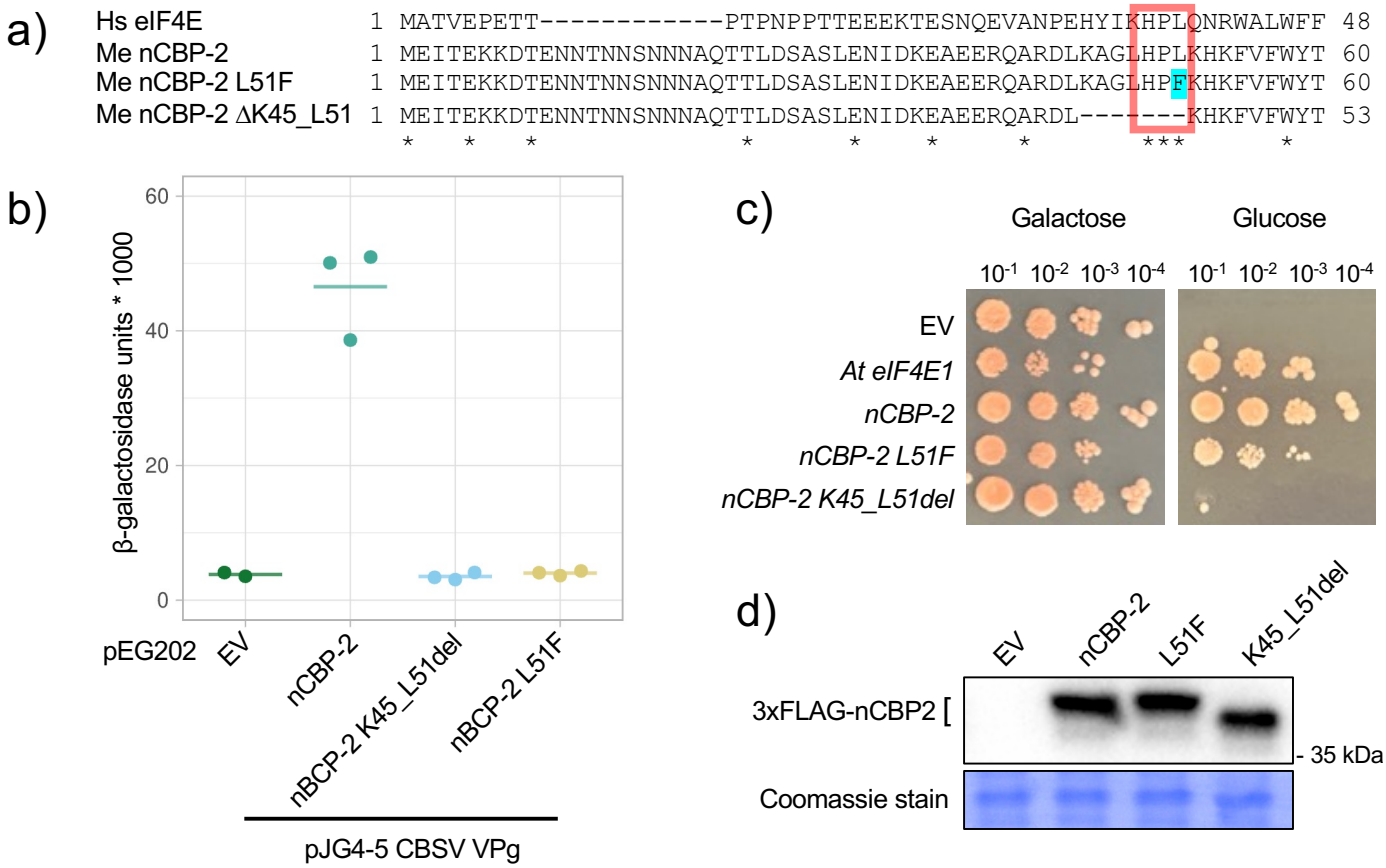

Fig. 5 Effects of HPL motif mutation on nCBP-2 affinity for CBSV VPg and translation initiation

a) Alignment of human eIF4E protein sequence with variants of cassava nCBP-2. The conserved HPL motif is boxed in red and the L51F mutation in nCBP-2 is highlighted in cyan. Asterisks denote conserved amino acid residues.
b) Quantitative yeast two-hybrid analysis of CBSV VPg interaction with nCBP-2 variants. Assays were performed after inducing VPg expression for five hours.
c) T93C *eif4e* yeast transformed with pG1.1 encoding *Arabidopsis eIF4E1* or cassava *nCBP-2* variants under the control of a constitutive promoter. nCBP-2 variants are N-terminally tagged with 3xFLAG. The T93C yeast strain harbors a plasmid encoding galactose-inducible and glucose-repressible yeast *eIF4E*.
d) Western blot analysis of nCBP-2 expression in yeast used in c). A segment of coomassie stained membrane is presented for loading control.

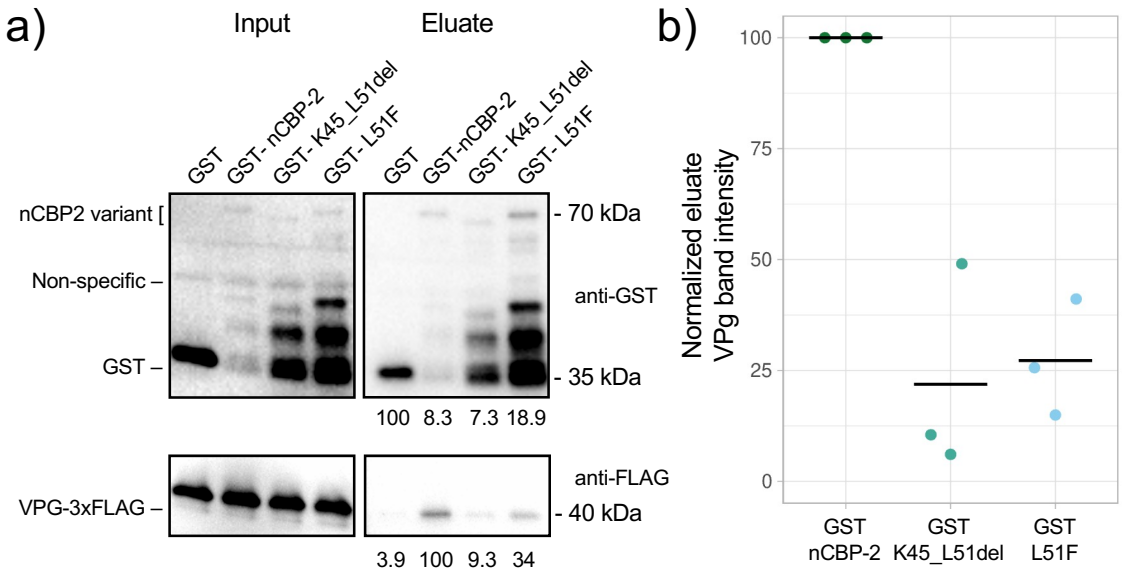

Fig. 6 nCBP-2^{K45_L51del} and nCBP-2^{L51F} exhibit reduced affinity for CBSV VPg, *in vitro*

a) GST pulldown experiment assessing the ability of GST-nCBP-2 variants to bind CBSV VPg. Full-length protein eluate band intensities are presented underneath the eluate western blots and are expressed relative to the sample with the strongest band intensity. Proteins were run on Tris-glycine SDS-PAGE gels. b) Analysis of eluate VPg band intensity across three GST-pulldown experiments. Band intensities are normalized to account for differing amounts of GST-fusion protein pulled down and expressed relative to VPg intensity in the GST-nCBP-2 sample.

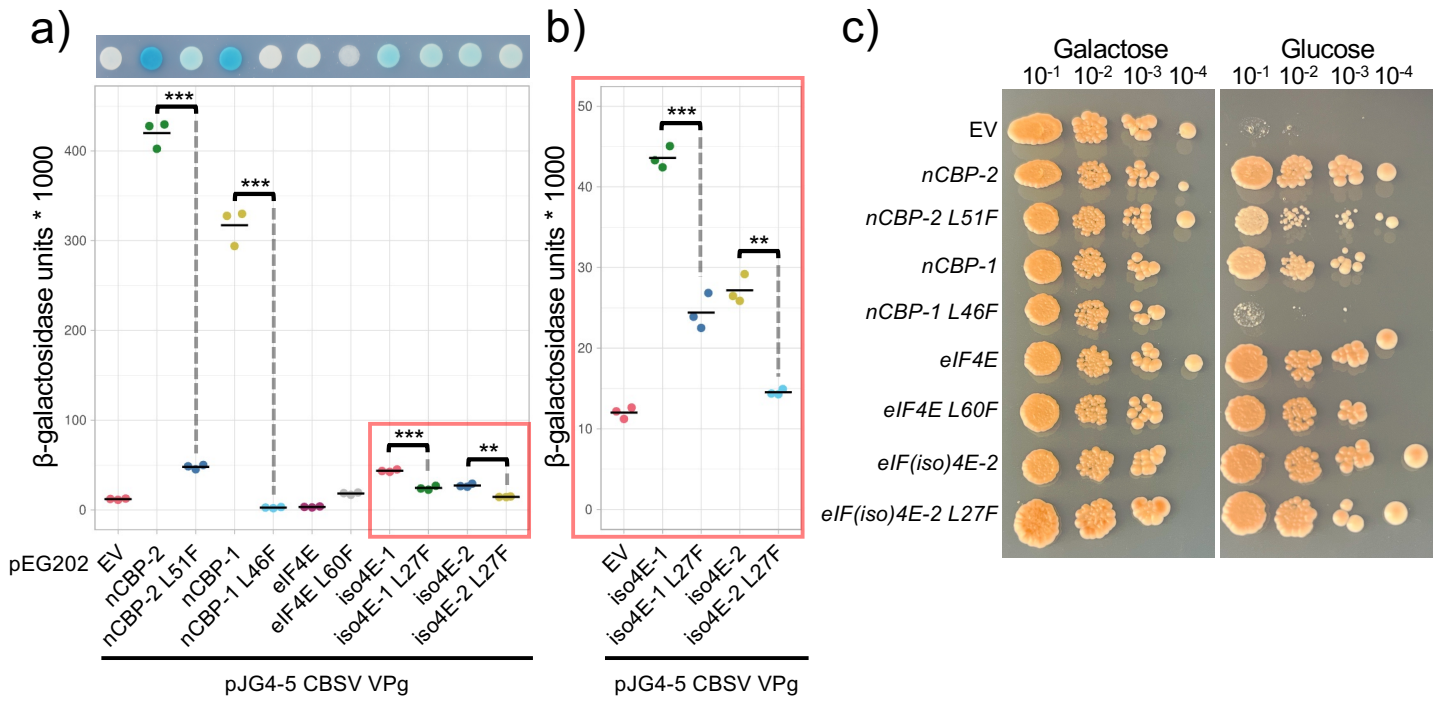

Fig. 7 Effects of mutating the HPL motif leucine in cassava *eIF4E* and *eIF(iso)4E*

a, b) Quantitative yeast two-hybrid analysis of CBSV VPg interaction with wild type cassava eIF4E-famiy proteins alongside HPL to HPF mutants. Assays were performed after growing yeast under VPg inducing conditions for 48 hours. Results for eIF(iso)4E-1 and -2 interaction with CBSV VPg in panel a), highlighted with a red box, are enlarged in panel b). Statistical differences were detected using a Welch's T-test with an alpha = 0.05. ** ≤ 0.01, *** ≤ 0.001.
c) T93C *eif4e* yeast complementation assay with wild-type and mutant *eIF4E*-family genes from cassava.